

H⁻ and He in a uniform magnetic field: Ground-state wave functions, energies, and binding energies for fields below 10⁹ G

Chang-Hwan Park and Anthony F. Starace

Behlen Laboratory of Physics, The University of Nebraska, Lincoln, Nebraska 68588-0111

(Received 5 July 1983)

Wave functions, energies, and binding energies for the lowest singlet states of H⁻ and He in uniform magnetic fields $B < 10^9$ G are calculated using an adiabatic approximation in hyperspherical coordinates. In computing the angular part of the wave functions, a coupled expansion in one-electron oblate spheroidal angle functions is used. In addition to contracting the two-electron wave function radially, the magnetic field is found to distort the angular part of the wave function mainly by reducing the ss 1S character of the state and replacing it with an sd 1D character. Results for energies and binding energies are comparable with those obtained in variational calculations. In order to compute the binding energies of H⁻ and He we have also calculated the binding energies of the ground states of H and He⁺ in uniform magnetic fields $B < 10^9$ G using the adiabatic oblate-spheroidal-coordinate method of Starace and Webster.

I. INTRODUCTION

The study of atomic hydrogen, or of hydrogenlike atoms, in a high uniform magnetic field has attracted increasing experimental and theoretical interest, as has been reviewed elsewhere.^{1,2} In addition to its applications to astrophysics³ and to solid-state physics,^{4,5} such study is of high theoretical interest in atomic physics because it requires new methods for treating the nonseparability of the Schrödinger equation for an electron in combined Coulomb and uniform magnetic fields.^{1,2} Two-electron and heavier atoms in high uniform magnetic fields are also of interest for their applications.^{3,5} Such atoms, however, have not been as well studied theoretically because they require a description of *correlated* electronic motion in combined Coulomb and uniform magnetic fields.

Much of the theoretical work which has been carried out for nonhydrogenic atoms has been concerned either exclusively or primarily with magnetic fields $B \gtrsim 10^9$ G which strongly influence the orbital motion of even ground-state atomic electrons, at least away from the atomic nucleus, and for which electron correlation effects are of less importance than magnetic field effects. Thus, studies⁶⁻⁸ have been carried out which have predicted quite novel atomic structures for heavy atoms in magnetic fields of order 10^{12} G, such as are thought to exist on neutron stars. For two-electron systems in such high magnetic fields, a number of specific calculations⁹⁻¹³ for the ground and low-excited states have been done employing approximations appropriate to such high fields such as use of cylindrical coordinate wave functions, etc.

Only a few calculations for two-electron systems have been designed to appropriately treat the region of magnetic field strengths $B \lesssim 10^9$ G for which electron correlation effects are dominant or at least comparable to magnetic interaction effects. Calculations¹⁴⁻¹⁷ for energy levels and spectral line strengths of He have been performed which treat the magnetic interaction terms perturbatively for

fields in the range 10^6 G $\lesssim B \lesssim 10^8$ G. Variational calculations¹⁸⁻²⁰ for H⁻ and He energy levels which use spherical coordinate trial functions have been done for fields in the range $0 \leq B \leq 10^{11}$ G. Recently, the 1S and 3S ground-state energies of the heliumlike systems He I, Si XIII, and Fe XXV have been calculated in this magnetic field region using both perturbative and Hartree-Fock approaches.²¹

We present here a detailed study of the effects of uniform magnetic fields $B < 10^9$ G on the two-electron wave functions, energies, and binding energies for the 1S ground states of H⁻ and He. In order to describe electron correlation effects as simply and as accurately as possible we provide here an adiabatic hyperspherical coordinate description of two-electron systems in uniform magnetic fields. Such hyperspherical adiabatic approximations have been shown, in the field-free case, to provide both qualitative insights and quantitatively accurate predictions for low-energy two-electron states.²²⁻²⁴ Furthermore, for the lowest states of a given symmetry these adiabatic approximations provide rigorous upper and lower bounds on the energies and binding energies.²⁵

A key approximation in our approach is that we represent the hyperspherical angle function as a truncated expansion in coupled one-electron oblate spheroidal angle functions.^{26,27} These functions have been shown²⁵ to provide an accurate description of one-electron motion in a uniform magnetic field; each of these functions implicitly includes a large amount of the l mixing which is an important feature of such motion. We show in this paper that such one-electron l mixing is the dominant magnetic field distortion of the angular part of the two-electron ground-state wave functions of H⁻ and He.

In Sec. II we present our hyperspherical coordinate formulation of two-electron systems in a uniform magnetic field. In Sec. III we describe the approximations used to solve the equations presented in Sec. II. In Sec. IV we show the magnetic field-induced changes in the angular and radial distribution of the two-electron wave functions.

We also present our results for the energies and the binding energies of H⁻ and He. In order to obtain the binding energies we have had to compute the energies of the one-electron systems H and He⁺ in a uniform magnetic field. We present these one-electron energies here also; they were obtained using the adiabatic oblate-spheroidal-coordinate method of Ref. 25. Finally, in Sec. V we present our conclusions.

II. EXACT FORMULATION

A. Schrödinger equation in hyperspherical coordinates

For singlet states, the Schrödinger equation in spherical coordinates for a two-electron system in combined Coulomb and uniform magnetic fields is²⁸

$$\sum_{i=1}^2 \left[-\frac{\hbar^2}{2m_e} \nabla_i^2 + \frac{|e|}{2m_e c} B L_{iz} + \frac{e^2}{8m_e c^2} B^2 r_i^2 \sin^2 \theta - \frac{Z e^2}{r_i} \right] \Psi(\vec{r}_1, \vec{r}_2) + \frac{e^2}{|\vec{r}_1 - \vec{r}_2|} \Psi(\vec{r}_1, \vec{r}_2) = E \Psi(\vec{r}_1, \vec{r}_2), \quad (1)$$

where the magnetic field B has been oriented along the z axis, L_{iz} is the z component of the orbital angular momentum operator for the i th electron, and m_e is the electron mass.²⁹ The operators in Eq. (1) are those for the kinetic energy, the linear Zeeman shift, the quadratic Zeeman shift, the nuclear Coulomb interaction, and the electron-electron Coulomb interaction. We shall use atomic units henceforth (i.e., $m_e = e = \hbar = 1$), introduce the strength parameter γ ,

$$\gamma \equiv B/2c = (2.12715 \times 10^{-10} \text{ a.u./G}) B(G), \quad (2)$$

and transform $|\vec{r}_1|$ and $|\vec{r}_2|$ to the hyperspherical coordinates R and α using

$$r_1 \equiv R \cos \alpha, \quad (3a)$$

$$r_2 \equiv R \sin \alpha. \quad (3b)$$

Then Eq. (1) becomes³⁰

$$\left[\frac{d^2}{dR^2} + \frac{5}{R} \frac{d}{dR} - \frac{\Lambda^2 + RC}{R^2} - \gamma^2 R^2 (\cos^2 \alpha \sin^2 \theta_1 + \sin^2 \alpha \sin^2 \theta_2) + 2E' \right] \Psi(R, \alpha, \hat{r}_1, \hat{r}_2) = 0. \quad (4)$$

In Eq. (4), Λ^2 is the generalized angular momentum operator,

$$\Lambda^2 \equiv -\frac{1}{\sin^2 \alpha \cos^2 \alpha} \frac{d}{d\alpha} \sin^2 \alpha \cos^2 \alpha \frac{d}{d\alpha} + \frac{\hat{L}_1^2}{\cos^2 \alpha} + \frac{\hat{L}_2^2}{\sin^2 \alpha}, \quad (5)$$

where \hat{L}_1 and \hat{L}_2 are the angular momentum operators for particles 1 and 2. The operator C in Eq. (4) is the sum of the nuclear and interelectron Coulomb interactions,

$$C \equiv -\frac{2}{(1 - \sin 2\alpha \cos \theta_{12})^{1/2}} + 2 \left[\frac{Z}{\cos \alpha} + \frac{Z}{\sin \alpha} \right], \quad (6)$$

and, lastly, E' is the total system energy reduced by the linear Zeeman energy,

$$E' \equiv E - \gamma M, \quad (7)$$

where M is the z component of the system's orbital angular momentum.

Following Macek,²² we write the two-electron wave function as a sum of products of radial and angular functions as follows:

$$\Psi_{E'}(R, \alpha, \hat{r}_1, \hat{r}_2) = (R^{5/2} \sin \alpha \cos \alpha)^{-1} \times \sum_{\mu} F_{\mu E'}(R) \Phi_{\mu}(R; \alpha, \hat{r}_1, \hat{r}_2). \quad (8)$$

Substituting Eq. (8) in Eq. (4) one finds that the channel function Φ_{μ} satisfies the following angular equation,

$$\left[\frac{d^2}{d\alpha^2} + RC - \frac{(\hat{L}_1^2 + \chi^2 \sin^2 \theta_1)}{\cos^2 \alpha} - \frac{(\hat{L}_2^2 + \eta^2 \sin^2 \theta_2)}{\sin^2 \alpha} \right] \Phi_{\mu} = U_{\mu}(R) \Phi_{\mu}, \quad (9)$$

where $U_{\mu}(R)$ is an eigenvalue and R is treated as a parameter. In Eq. (9) we have defined the variables χ and η , where

$$\chi \equiv \gamma R^2 \cos^2 \alpha, \quad (10a)$$

$$\eta \equiv \gamma R^2 \sin^2 \alpha, \quad (10b)$$

for reasons to be discussed below. Note that Eq. (9) is independent of the system energy E' ; Φ_{μ} describes the angular character of a channel μ of two-electron states whose individual members differ only in their radial behavior. The channel functions are orthonormal at each R ,

$$(\Phi_{\mu}, \Phi_{\mu'}) \equiv \int_0^{\pi/2} d\alpha \int d\hat{r}_1 \int d\hat{r}_2 \Phi_{\mu}^*(R; \alpha, \hat{r}_1, \hat{r}_2) \times \Phi_{\mu'}(R; \alpha, \hat{r}_1, \hat{r}_2) = \delta_{\mu\mu'}. \quad (11)$$

The radial functions $F_{\mu E'}(R)$ satisfy the following coupled set of equations:²²

$$\left[\frac{d^2}{dR^2} + \frac{U_{\mu}(R) + \frac{1}{4}}{R^2} + 2E' \right] F_{\mu E'}(R) + \sum_{\mu'} \left[\left[\Phi_{\mu}, \frac{\partial^2 \Phi_{\mu'}}{\partial R^2} \right] F_{\mu' E'} + 2 \left[\Phi_{\mu}, \frac{\partial \Phi_{\mu'}}{\partial R} \right] \frac{\partial F_{\mu' E'}}{\partial R} \right] = 0, \quad (12)$$

where the coupling matrix elements between different channels μ and μ' are angular matrix elements of the radial derivative operators. Differentiation of the orthonormality relation (11) with respect to R shows that the first derivative matrix elements are antisymmetric,

$$\left[\Phi_{\mu'}, \frac{\partial \Phi_{\mu'}}{\partial R} \right] = - \left[\frac{\partial \Phi_{\mu'}}{\partial R}, \Phi_{\mu'} \right], \quad (13)$$

and, hence, the diagonal elements vanish,

$$\left[\Phi_{\mu'}, \frac{\partial \Phi_{\mu'}}{\partial R} \right] = 0. \quad (14)$$

Differentiation of Eq. (14) with respect to R shows that

$$\left[\Phi_{\mu'}, \frac{\partial^2 \Phi_{\mu'}}{\partial R^2} \right] = - \left[\frac{\partial \Phi_{\mu'}}{\partial R}, \frac{\partial \Phi_{\mu'}}{\partial R} \right] \leq 0, \quad (15)$$

i.e., the diagonal second derivative elements are negative definite.

B. Oblate-spheroidal angle function expansion

In the absence of a uniform magnetic field, $\gamma = \chi = \eta = 0$, and the standard procedure for solving Eq. (9) for the channel function and its eigenvalue at each R is to make an expansion in the eigenstates of \hat{L}_1^2 and \hat{L}_2^2 , i.e., in spherical harmonics. Thus, Macek writes²²

$$\Phi_{\mu}^{LM} \equiv \sum_{l_1 l_2} A_{l_1 l_2 LM}^{\mu}(R; \alpha) \mathcal{Y}_{l_1 l_2 LM}(\hat{r}_1, \hat{r}_2), \quad (16)$$

where

$$\mathcal{Y}_{l_1 l_2 LM}(\hat{r}_1, \hat{r}_2) = \sum_{m_1 m_2} Y_{l_1 m_1}(\hat{r}_1) Y_{l_2 m_2}(\hat{r}_2) \times \langle l_1 m_1 l_2 m_2 | LM \rangle, \quad (17)$$

where the coefficient in Eq. (17) is a Clebsch-Gordon coefficient, and where the coefficient in Eq. (16) must be obtained numerically at each R by solving a differential equation in α .

In the presence of a uniform magnetic field, the numerators of the $\cos^{-2}\alpha$ and $\sin^{-2}\alpha$ terms in Eq. (9) may be considered as operators in θ_1 and θ_2 , respectively, with χ and η regarded as parameters. These operators have as eigenstates the oblate-spheroidal angle functions^{26,27} $g_{\nu_1 m_1}(\chi; \theta_1)$ and $g_{\nu_2 m_2}(\eta; \theta_2)$, where

$$\left[-\frac{1}{\sin\theta_1} \frac{d}{d\theta_1} \left[\sin\theta_1 \frac{d}{d\theta_1} \right] + \frac{m_1^2}{\sin^2\theta_1} + \chi^2 \sin^2\theta_1 \right] g_{\nu_1 m_1}(\chi; \theta_1) = V_{\nu_1 m_1}(\chi) g_{\nu_1 m_1}(\chi; \theta_1) \quad (18)$$

and $g_{\nu_2 m_2}(\eta; \theta_2)$ satisfies a similar equation. Note that $g_{\nu_1 m_1}$ depends only on $|m_1|$ since only m_1^2 appears in Eq. (18). When $\chi \rightarrow 0$ due either to vanishing magnetic field B or to vanishing $r_1 = R \cos\alpha$, then the oblate spheroidal angle function and its eigenvalue have the following limit behaviors,

$$g_{\nu_1 m_1}(\chi; \theta_1) \xrightarrow{\chi \rightarrow 0} \Theta_{\nu_1 m_1}(\cos\theta_1), \quad (19a)$$

$$V_{\nu_1 m_1}(\chi) \xrightarrow{\chi \rightarrow 0} \nu_1(\nu_1 + 1), \quad (19b)$$

i.e., $g_{\nu_1 m_1}$ and $V_{\nu_1 m_1}$ become an eigenstate and an eigen-

value of \hat{L}_1^2 , respectively, with orbital angular momentum quantum number ν_1 . The function $\Theta_{\nu_1 m_1}(\cos\theta_1)$ is simply related to a spherical harmonic:

$$Y_{\nu_1 m_1}(\theta_1, \phi_1) = \Theta_{\nu_1 m_1}(\cos\theta_1) \exp(im_1 \phi_1) / \sqrt{2\pi}. \quad (20)$$

For $\chi > 0$, on the other hand, $g_{\nu_1 m_1}(\chi; \theta_1)$ represents an expansion in orbital momentum eigenstates $\Theta_{lm}(\cos\theta)$,

$$g_{\nu m}(\chi; \theta) = \sum'_{l > |m|} D_l^{\nu m}(\chi) \Theta_{lm}(\cos\theta), \quad (21)$$

where the prime on the summation indicates that only those l having the same parity as ν are summed. The coefficients have the expected limit behavior,

$$D_l^{\nu m}(\chi) \xrightarrow{\chi \rightarrow 0} \delta_{l\nu}. \quad (22)$$

As shown in Ref. 25, the oblate-spheroidal angle functions provide a good representation of the angular part of a low-energy one-electron wave function for magnetic fields $B < 10^9$ G because, as in Eq. (21), they implicitly include a large amount of the l mixing which is a characteristic of the motion of an electron in a uniform magnetic field. For this reason, we generalize in the case of a uniform magnetic field the representation in Eqs. (16) and (17) for the channel function Φ_{μ} by representing it as an expansion in coupled oblate-spheroidal angle functions instead of in ordinary spherical harmonics,

$$\Phi_{\mu}^M = \sum_{\nu_1 \nu_2 \lambda} A_{\nu_1 \nu_2 \lambda M}^{\mu}(R; \alpha) \mathcal{Y}_{\nu_1 \nu_2 \lambda M}(\chi, \eta; \hat{r}_1, \hat{r}_2), \quad (23)$$

where

$$\mathcal{Y}_{\nu_1 \nu_2 \lambda M}(\chi, \eta; \hat{r}_1, \hat{r}_2) = \sum_{m_1 m_2} g_{\nu_1 m_1}(\chi; \theta_1) [\exp(im_1 \phi_1) / \sqrt{2\pi}] g_{\nu_2 m_2}(\eta; \theta_2) \times [\exp(im_2 \phi_2) / \sqrt{2\pi}] \langle \nu_1 m_1 \nu_2 m_2 | \lambda M \rangle. \quad (24)$$

Note that there is a sum over λ since this is not a conserved quantum number in the presence of a uniform magnetic field. Note also that because of its dependence on χ and η (cf. Eq. 10), $\mathcal{Y}_{\nu_1 \nu_2 \lambda M}$ in Eq. (24) depends on R and α . This dependence complicates the differential equation for the coefficients $A_{\nu_1 \nu_2 \lambda M}^{\mu}$ as compared to the field-free case. This added complication, however, will be compensated in approximate calculations by the better representation provided by the oblate-spheroidal angle functions, which permits a straightforward means of truncating the expansion over ν_1 , ν_2 , and λ , as discussed in Sec. III.

Using the representation for the channel function Φ_{μ}^M in Eq. (23), Eq. (9) may be reduced to a differential equation in α for the expansion coefficients $A_{\nu_1 \nu_2 \lambda M}^{\mu}$. One substitutes Eq. (23) in Eq. (9), multiplies from the left by the complex conjugate of Eq. (24), and integrates over \hat{r}_1 and \hat{r}_2 , taking note of Eq. (18) for the oblate-spheroidal angle functions as well as of their orthonormality, e.g.,

$$(g_{\nu_1 m_1}, g_{\nu_1' m_1'}) \equiv \int_0^{\pi} g_{\nu_1 m_1}(\chi, \theta_1) g_{\nu_1' m_1'}(\chi, \theta_1) \sin\theta_1 d\theta_1 = \delta_{\nu_1 \nu_1'}. \quad (25)$$

The result is

$$\begin{aligned}
& \left[\frac{d^2}{d\alpha^2} - U_\mu(R) \right] A_{\nu_1\nu_2\lambda M}^\mu(R; \alpha) \\
&= \sum_{\lambda'} \left[\sum_{m_1 m_2} \langle \nu_1 m_1 \nu_2 m_2 | \lambda M \rangle \left[\frac{V_{\nu_1 m_1}(\chi)}{\cos^2 \alpha} + \frac{V_{\nu_2 m_2}(\eta)}{\sin^2 \alpha} \right] \langle \nu_1 m_1 \nu_2 m_2 | \lambda' M \rangle \right] A_{\nu_1\nu_2\lambda' M}^\mu(R; \alpha) \\
&- \sum_{\nu_1' \nu_2' \lambda'} (RC_{\nu_1\nu_2\lambda, \nu_1'\nu_2'\lambda'} + X_{\nu_1\nu_2\lambda, \nu_1'\nu_2'\lambda'}) A_{\nu_1'\nu_2'\lambda' M}^\mu(R; \alpha) - \sum_{\nu_1' \nu_2' \lambda'} W_{\nu_1\nu_2\lambda, \nu_1'\nu_2'\lambda'} \frac{\partial}{\partial \alpha} A_{\nu_1'\nu_2'\lambda' M}^\mu(R; \alpha). \quad (26)
\end{aligned}$$

In Eq. (26) the first summation on the right contains the oblate-spheroidal eigenvalues $V_{\nu_1 m_1}$ and $V_{\nu_2 m_2}$ which represent, through χ and η , R - and α -dependent potentials for one-electron motion in a uniform magnetic field. When $B \rightarrow 0$ the potentials $V_{\nu_1 m_1}$ and $V_{\nu_2 m_2}$ become constants independent of m_1 or m_2 and the sum over m_1 and m_2 may be performed to obtain $\delta_{\lambda\lambda'}$. Similarly, when one of the electrons moves close to the nucleus so that either $r_1 = R \cos \alpha$ or $r_2 = R \sin \alpha$ becomes ≈ 0 , then the corresponding potential becomes a constant and for that term the sum over m_1 and m_2 may be performed to obtain $\delta_{\lambda\lambda'}$. Otherwise, one sees that the one-electron oblate-spheroidal potentials, while preserving the oblate-spheroidal quantum numbers ν_1 and ν_2 , do lead to a certain amount of λ mixing. The operator C has been defined in Eq. (6); the matrices X and W arise due to the α dependence of the oblate-spheroidal angle functions. Expressions for the matrices C , S , and W are given in Appendix A.

III. APPROXIMATIONS EMPLOYED

Both the angular differential equation (26) and the radial differential equation (12) have the form of an infinite set of coupled differential equations. In seeking suitable approximations we have been guided on the one hand by previous work on the hydrogen atom in a uniform magnetic field.²⁵ This work shows that for low-lying bound states, a single oblate-spheroidal angle function is a good representation of the angular part of the single electron's wave function up to fields of order $B \lesssim 10^9$ G. This implies, in other words, that use of the oblate-spheroidal eigenvalue $V_{\nu m}$ and its corresponding eigenfunction $g_{\nu m}$ are sufficient in this field strength regime and that consideration of the off-diagonal coupling matrix elements involving derivatives of $g_{\nu m}$ with respect to the parameters χ and η , such as those that occur implicitly in the definition of the matrices in Appendix A, is less important. On the other hand, we have also been guided by previous work on the separable or adiabatic approximation in hyperspherical coordinates.²²⁻²⁴ This work shows that both quantitatively and qualitatively the adiabatic approximation in hyperspherical coordinates is accurate for the lowest states of two-electron systems. Based on this previous experience, we have therefore made the following three approximations in solving Eqs. (12) and (26).

A. Truncation of the basis set

In the field-free case, we have obtained convergence of hyperspherical adiabatic energy eigenvalues for the 1S

ground states of H⁻ and He using the (l_1, l_2) pairs (0,0), (1,1), (2,2), and (3,3) in Eq. (16). Since we expect magnetic field effects near the nucleus to be negligible, we have chosen to represent the channel function in Eq. (23) in the presence of a magnetic field in such a way that for either $B \rightarrow 0$ or $R \rightarrow 0$ Eq. (23) reduces exactly to the field-free channel function in Eq. (16). Thus, we have restricted the summation in Eq. (23) as follows: We require that $\lambda' = L = 0$ and that the pairs (ν_1, ν_2) have the same values, i.e., (0,0), (1,1), (2,2), and (3,3), as in the field-free case. With this choice, Eq. (23) does reduce to Eq. (16) as either R or B becomes small due to the oblate-spheroidal angle function's becoming the θ part of a spherical harmonic under these circumstances [cf. Eqs. (19a), (20), and (24) with Eq. (17)].

It is important to note that, in restricting λ' to zero, we are *not* forcing the total angular momentum of the system to be zero. Furthermore, in choosing the (ν_1, ν_2) pairs to be (0,0), (1,1), (2,2), and (3,3), we are not restricting the one-electron orbital angular momenta to these values. This is because ν_1 , ν_2 , and λ are *not* orbital angular momenta: ν_1 and ν_2 are oblate-spheroidal quantum numbers which equal one-electron orbital angular momentum quantum number only near the nucleus or in zero magnetic field; λ happens to be a quantum number obtained by combining ν_1 and ν_2 as if they were orbital angular momenta. In fact, we find that the most significant effect of the magnetic field on the angular part of the two-electron wave function is to introduce a component with $l_1 = 0$, $l_2 = 2$, and $L = 2$ which, while not obviously contained in our basis set (since $\lambda = 0$ and ν_1 and ν_2 are restricted to pairs with $\nu_1 = \nu_2$), is nevertheless included due to the l mixing implicitly accounted for by our use of oblate-spheroidal angle functions.

B. Perturbative treatment of angular equation matrix elements

Since we have restricted $\lambda = \lambda' = 0$, the three matrices in Eq. (26) have elements which may be written as $C_{\nu_1\nu_2, \nu_1'\nu_2'}$, $X_{\nu_1\nu_2, \nu_1'\nu_2'}$, and $W_{\nu_1\nu_2, \nu_1'\nu_2'}$. As shown in Eq. (A1), the only part of $C_{\nu_1\nu_2, \nu_1'\nu_2'}$ which is changed by the magnetic field is the interelectron Coulomb interaction; the nuclear Coulomb interaction is unaffected. But the electron-electron interaction is only large near the nucleus, where magnetic field effects are small. For this reason a perturbative treatment of the magnetic field effects on this matrix element is appropriate.

As shown in Eqs. (A2) and (A3), $X_{\nu_1\nu_2, \nu'_1\nu'_2}$ and $W_{\nu_1\nu_2, \nu'_1\nu'_2}$ are dependent on first- and second-derivative coupling matrix elements of the oblate-spheroidal harmonics. These latter coupling matrix elements, however, are small unless the parameters χ and η in Eq. (10) become significantly greater than unity. This occurs, for the field strengths considered for H^- and He here, only in the tail of the two-electron wave function. Hence, the magnetic field effects may also be treated perturbatively here.

For these reasons we have made the following perturbative approximation: We write the oblate-spheroidal expansion coefficients $D_l^{ym}(\chi)$ and $D_l^{ym}(\eta)$ [cf. Eqs. (21) and (22)] as

$$D_l^{ym} = \delta_{lv} + \Delta_l^{ym}. \quad (27)$$

We then calculate the matrices in Appendix A only to first order in the Δ coefficients. The results for these matrices are given in Appendix B.

From Eq. (27) we see that a perturbative approximation will work provided $\Delta_l^{ym} \ll 1$. Our calculations show that $\Delta_l^{ym} \leq 0.1$ for the fields and states considered in this paper. Specifically, for H^- in a field of 10^8 G, $\Delta_l^{ym} \leq 0.1$ for radial coordinate values $R \leq 12$; for He in a field of 10^9 G, $\Delta_l^{ym} \leq 0.1$ for radial coordinate values $R \leq 4$. For lower magnetic field strengths this condition on Δ_l^{ym} would be satisfied for larger R values. Note that, for R values larger than those indicated, the H^- and He wave functions are exponentially decaying and so values $\Delta_l^{ym} > 0.1$ occur only in regions of coordinate space where the probability of finding an electron is small.

C. Adiabatic approximations to the radial equation (12)

In the adiabatic or separable approximation to the radial Eq. (12), one drops all off-diagonal coupling matrix elements:²²

$$\left[\frac{d^2}{dR^2} + \frac{U_\mu(R) + \frac{1}{4}}{R^2} + \left[\Phi_\mu, \frac{\partial^2 \Phi_\mu}{\partial R^2} \right] + 2E'_U \right] F_{\mu E'}(R) = 0. \quad (28)$$

The subscript U on the energy eigenvalue indicates that for the lowest energy state of a given symmetry, E'_U is a rigorous upper bound on the true energy.²⁵ If one drops the diagonal coupling matrix element, Eq. (28) becomes

$$\left[\frac{d^2}{dR^2} + \frac{U_\mu(R) + \frac{1}{4}}{R^2} + 2E'_L \right] F_{\mu E'}(R) = 0. \quad (29)$$

Here the subscript L on the energy eigenvalue indicates that for the lowest energy state of a given symmetry, E'_L is

$$\langle \mathcal{Y}_{i_1 l_2 L 0} | \Phi_\mu^{M=0} \rangle = \sum_{\nu_1} A_{\nu_1 \nu_1 00}^\mu(R; \alpha) \left[\frac{2L+1}{2\nu_1+1} \right]^{1/2} (-1)^{\nu_1} N_{l_1 l_2} \\ \times \sum_{m_1} [D_{l_1}^{\nu_1 m_1}(\chi) D_{l_2}^{\nu_1 m_1}(\eta) + (-1)^i D_{l_2}^{\nu_1 m_1}(\chi) D_{l_1}^{\nu_1 m_1}(\eta)] \begin{pmatrix} l_1 & l_2 & L \\ m_1 & -m_1 & 0 \end{pmatrix} (-1)^{m_1}. \quad (32)$$

a rigorous lower bound on the true energy.²⁵

Note that E'_U is to be compared with the results of variational calculations. Furthermore, E'_U is generally to be preferred to E'_L since one may show that the diagonal coupling term in Eq. (28) is necessary in order that $F_{\mu E'}(R)$ has the proper asymptotic form.²² The pair of values E'_U and E'_L provide not only bounds on the true energy but also an indication of the possible effect of the neglected off-diagonal coupling matrix elements.

IV. RESULTS AND DISCUSSION

In the adiabatic approximation discussed in Sec. III C, the two-electron wave function is represented as [cf. Eq. (8)]

$$\Psi_{E'}(R, \alpha, \hat{r}_1, \hat{r}_2) \approx (R^{5/2} \sin \alpha \cos \alpha)^{-1} F_{\mu E'}(R) \\ \times \Phi_\mu^M(R; \alpha, \hat{r}_1, \hat{r}_2), \quad (30)$$

where μ identifies the channel of two-electron states under consideration and E' gives the reduced energy of a particular state in that channel. The superscript M on the channel function simply makes explicit the fact that the z component of orbital angular momentum is a conserved quantum number. For the H^- and He ground states considered here, $M=0$. We discuss, in turn, the effects of a uniform magnetic field on the channel function Φ_μ , the radial function $F_{\mu E'}$, and the energy E' as well as the binding energy. Although we present wave function results only for H^- , our results for He are similar.

A. Angular distortion of the two-electron wave function

The channel function Φ_μ^M in Eq. (30) is represented by Eqs. (23) and (24). Its expansion coefficients are obtained by solving the eigenvalue equation (26) using the approximations discussed in Secs. III A and III B above. In order to display the effect of the magnetic field clearly we have projected the channel function Φ_μ^M onto the following set of orbital angular momentum basis states:

$$\mathcal{Y}_{i_1 l_2 L 0} = N_{l_1 l_2} \left[\mathcal{Y}_{l_1 l_2 L 0}(\hat{r}_1, \hat{r}_2) \right. \\ \left. + (-1)^{i+l_1+l_2-L} \mathcal{Y}_{l_2 l_1 L 0}(\hat{r}_1, \hat{r}_2) \right], \quad (31a)$$

where

$$N_{l_1 l_2} = 2^{-1} \delta_{l_1 l_2} + 2^{-1/2} (1 - \delta_{l_1 l_2}), \quad (31b)$$

and the coupled spherical harmonics appearing in Eq. (31a) are defined in Eq. (17). The index i takes the values 0 and 1 for symmetric and antisymmetric combinations of the coupled spherical harmonics. For $l_1=l_2$, of course, only the symmetric combination is nonzero.

The result of this projection is

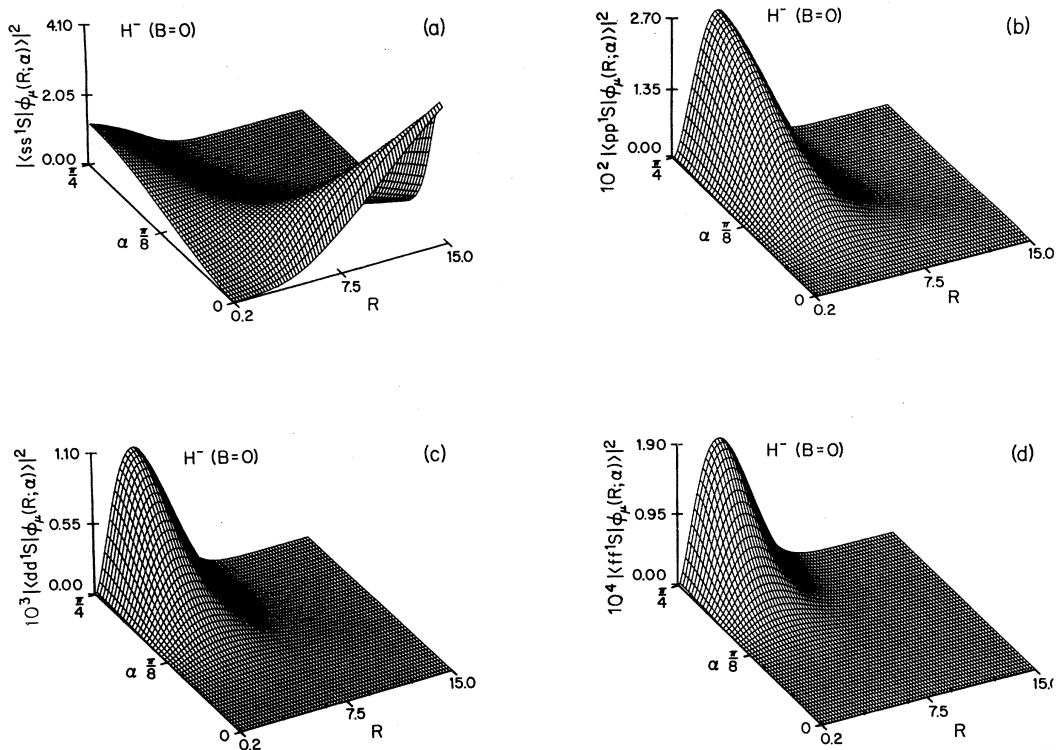


FIG. 1. Probability (per unit length in α) for the angular momentum state l^1S in the singlet ground state of H^- for $B=0$: (a) $l=0$; (b) $l=1$; (c) $l=2$; (d) $l=3$. Note multiplication by factors of 10^2 , 10^3 , and 10^4 in Figs. (b), (c), and (d), respectively.

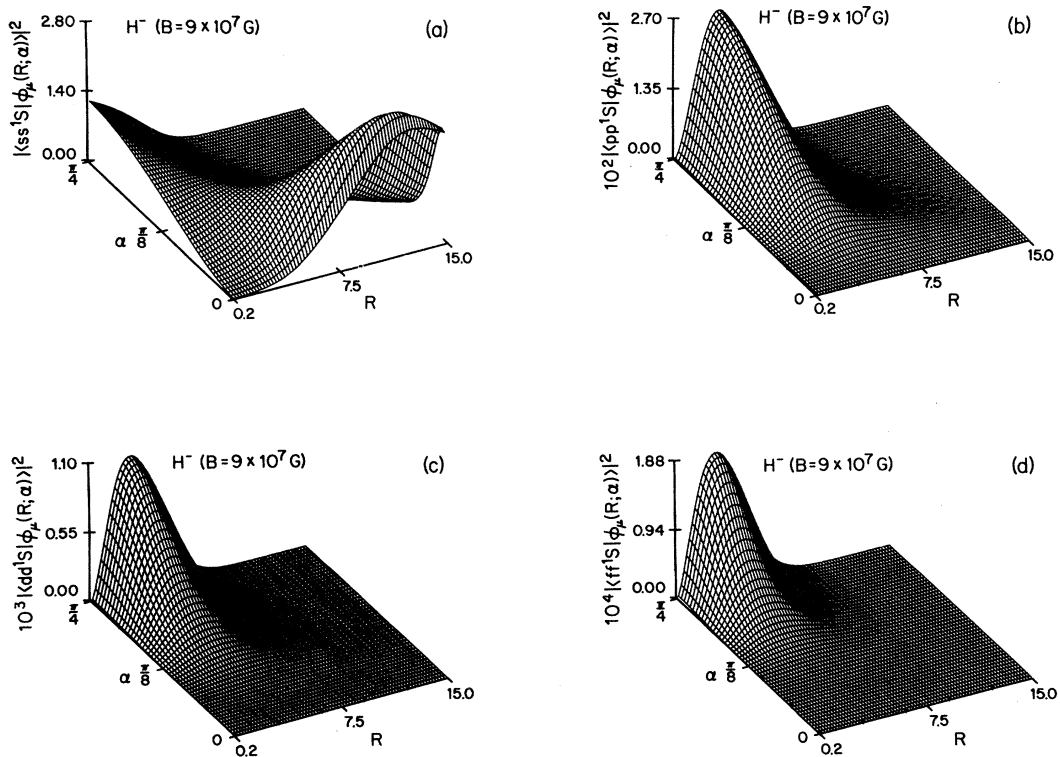


FIG. 2. Same as Fig. 1 for $B=9 \times 10^7$ G.

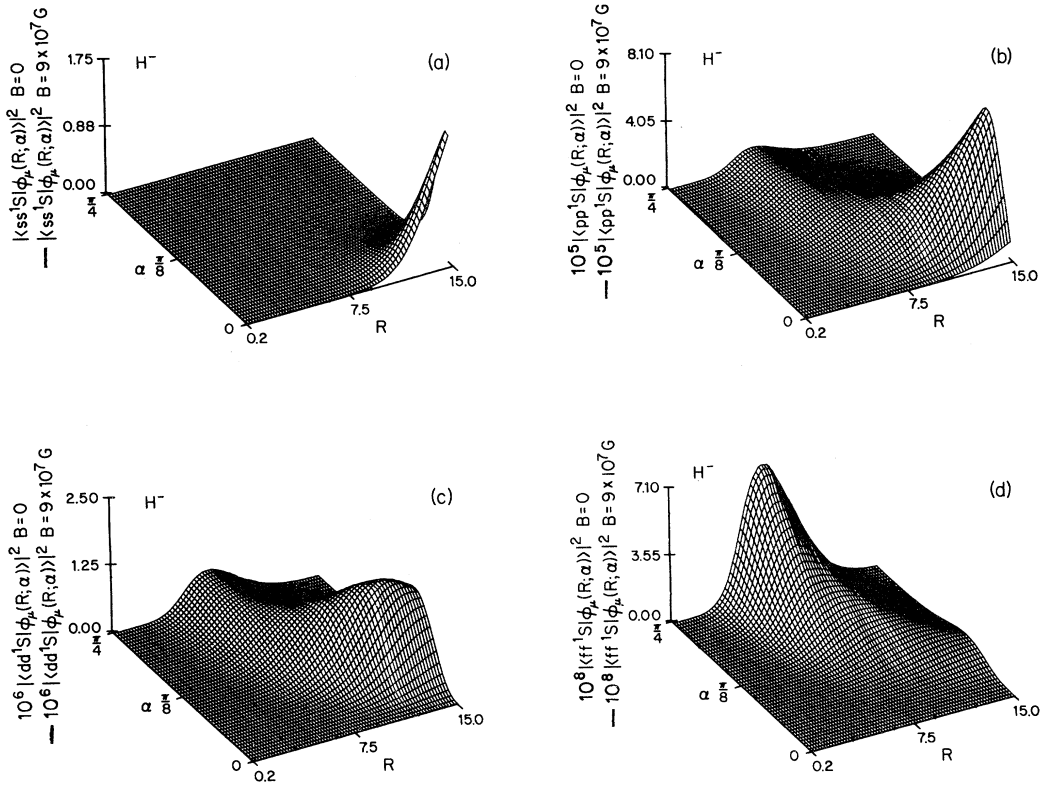


FIG. 3. Difference of corresponding probabilities in Figs 1 and 2.

Equation (32) indicates that Φ_μ^M has no component with odd L . This follows from three facts: l_1 and l_2 must have the same parity for the ground states considered here; the D_l^m coefficients depend only on $|m|$; if L is odd, the $3j$ coefficient is zero for $m=0$ and the sum of the two coefficients with values $m = \pm |m|$ is zero. [A similar analysis of each term in Eq. (26) shows that the $\lambda=M=0$ state couples only to states with even λ' values.] The square of the absolute value of Eq. (32) represents at each R the probability, per unit length in α , of the channel μ 's having the angular momentum character of a symmetric ($i=0$) or antisymmetric ($i=1$) ($l_1 l_2 L M=0$) state. This follows from the normalization of the channel functions Φ_μ in Eq. (11). When $\chi=\eta=0$, use of Eq. (22) allows the summation over m_1 to be performed analytically to obtain

$$\langle \mathcal{Y}_{i l_1 l_2 L O} | \Phi_\mu^{M=0} \rangle_{\chi, \eta \rightarrow 0} \rightarrow A_{l_1 l_2 00}^\mu(R, \alpha) \delta_{l_1 l_2} \delta_{L O} \delta_{i 0}. \quad (33)$$

In Fig. 1 we consider the $B=0$ case first, showing the absolute square of Eq. (33) in R and α space for the four largest angular momentum components of the lowest 1S channel function Φ_μ of H^- . In interpreting this and subsequent figures, recall Eq. (3): The region near $\alpha=\pi/4$ is where $r_1 \approx r_2$ while the region near $\alpha=0$ is where $r_1 \approx R$, $r_2 \approx 0$. (The symmetric region $\pi/4 \leq \alpha \leq \pi/2$ is not shown.) The striking feature of Fig. 1 is that, whereas near $\alpha=\pi/4$ the ll^1S components with $l>0$ make some contribution, they do not contribute significantly near

$\alpha=0$; for large R , in particular, the state has predominantly ss^1S character focused on an increasingly smaller region near $\alpha=0$.

In Fig. 2 we show the same channel function Φ_μ of H^- in a magnetic field $B=9 \times 10^7$ G. This time we plot the absolute square of Eq. (32) showing again the ll^1S components with $l=0, 1, 2$, and 3. The only significant change from the field-free case in Fig. 1 is in the ss^1S component, which is markedly decreased at large R . This loss of probability is even clearer in Fig. 3, in which we have plotted the difference in the probabilities in Figs. 1 and 2.

Figure 4 shows that the missing probability in Fig. 3(a) does not appear in states of the form ll^1L . We have plotted all such states for $l=0, 1, 2$, and 3 and L = even. These states have probabilities less than 10^{-7} per unit length in α . Notice that what probability there is in these channels appears only for large R .

Figure 5 shows exactly where all of the missing probability has gone. Here, for the first time, we show the probabilities that Φ_μ has components with $l_1 \neq l_2$. Since l_1 and l_2 must have the same parity, the three cases shown are the only ones permitted for $l_1, l_2 \leq 3$. We see that Fig. 5(a) for the symmetric ($i=0$) sd^1D probability is identical in shape to Fig. 3(a) for the missing ss^1S probability and has exactly one-half the probability. Not shown, because they are identical to Fig. 5, are the antisymmetric ($i=1$) probabilities for the same $l_1 l_2^1L$ states. The sum of the

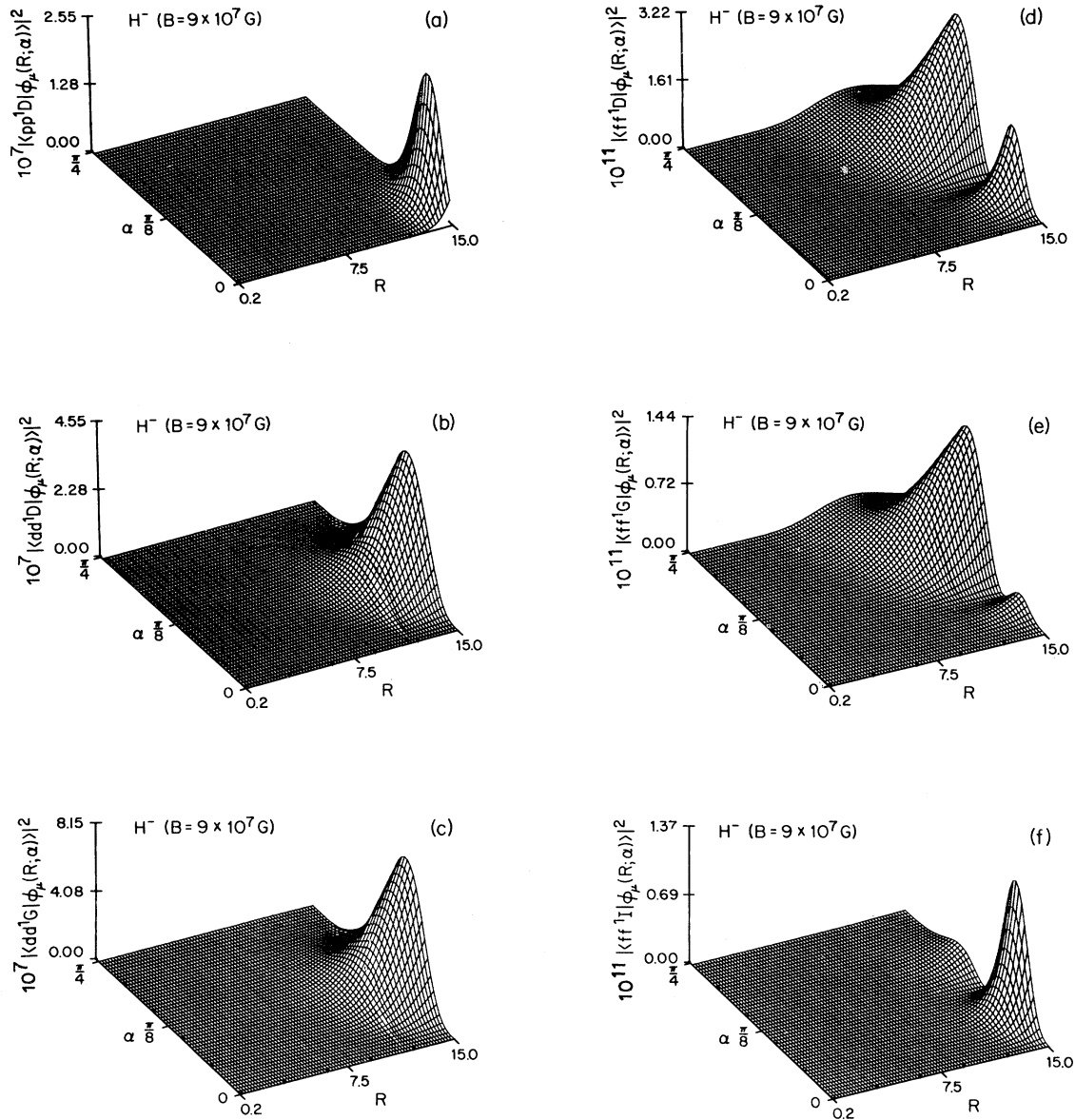


FIG. 4. Probability (per unit length in α) for the angular momentum state l^1L in the singlet ground state of H^- for $B = 9 \times 10^7 G$: (a) $l=1, L=2$; (b) $l=2, L=2$; (c) $l=2, L=4$; (d) $l=3, L=2$; (e) $l=3, L=4$; (f) $l=3, L=6$.

symmetric and antisymmetric sd^1D probabilities exactly equals the missing ss^1S probability. This implies that for the ground states of H^- (shown) and He (not shown) the main angular distortion of the wave function by an external uniform magnetic field is essentially a *one-electron transition* $s \rightarrow d$ of one of the electrons when it is far from the nucleus and the other electron is left behind (i.e., $r_1 \approx R \gg r_2 \approx 0$).

B. Radial distortion of the two-electron wave function

Our results for the He and H^- ground-state radial wave functions $F_{\mu E}(R)$ obtained by solving the hyperspherical adiabatic equation (28) are shown in Fig. 6. For H^- this wave function is computed for $B = 9 \times 10^7 G$ while that

for He is computed for $B = 3 \times 10^8 G$. One sees that the magnetic field compresses the radial wave function slightly to lower R values due to the quadratic Zeeman interaction. Specifically, as the parameters χ and η increase at large R [cf. Eq. (10)], the oblate-spheroidal eigenvalues increase [cf. Eq. (18)]. These, in turn, lead to an increase in $-U_\mu(R)$ [cf. Eq. (26)] at large R , which means that the effective potential seen by $F_\mu(R)$ increases [cf. Eq. (28)] causing the observed compression to lower values of R .

C. Ground-state energies and binding energies

We have calculated rigorous upper (lower) bounds on the lowest singlet state energies for H^- and He by solving Eq. (28) [Eq. (29)]. The binding energies $I(H^-)$ and $I(He)$

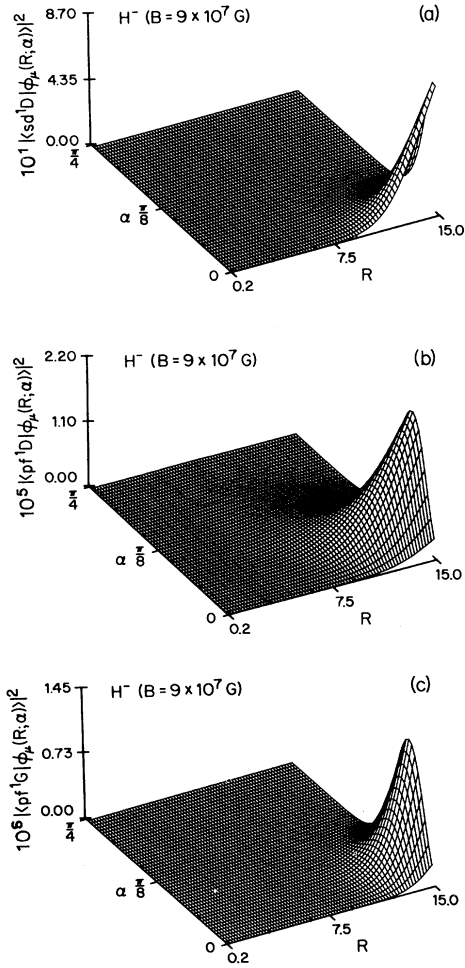


FIG. 5. Same as Fig. 4 for symmetric $l_1 l_2 {}^1L$ states: (a) $l_1=0$, $l_2=2$, $L=2$; (b) $l_1=1$, $l_2=3$, $L=2$; (c) $l_1=1$, $l_2=3$, $L=4$.

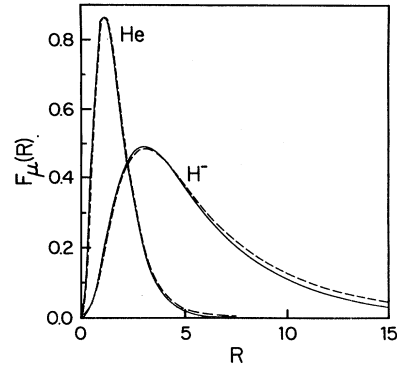


FIG. 6. Hyperspherical adiabatic radial wave functions for the singlet ground states of He ($B=3 \times 10^8$ G) and H^- ($B=9 \times 10^7$ G).

for the *singlet* state are obtained from the following equations:

$$E(H^-) + I(H^-) = E(H) + \gamma, \quad (34a)$$

$$E(\text{He}) + I(\text{He}) = E(\text{He}^+) + \gamma. \quad (34b)$$

These equations mean that when we just ionize the two-electron system we obtain the energy of the one-electron system in the same magnetic field plus an electron infinitely far away in the lowest Landau level³¹ having energy γ [cf. Eq. (2)]. Now for the one-electron system,²⁵

$$E(H) = -I(H) + \gamma, \quad (35a)$$

$$E(\text{He}^+) = -I(\text{He}^+) + \gamma. \quad (35b)$$

Further, if we follow the practice of Refs. 18–20 of referring the singlet state binding energy to the *triplet* state threshold, which is an energy -2γ lower due to the fact

TABLE I. Ground-state energy of H^- , $E(H^-)$, binding energy of H, $I(H)$, and binding energy of H^- , $I(H^-)$, in a uniform magnetic field.

γ^a (a.u.)	B (10^7 G)	$E(H^-)$ (a.u.)		$I(H)$ (a.u.)		$I(H^-)$ (a.u.)		Variational HOSCR ^b
		Present adiabatic results		Present adiabatic results		Present adiabatic results		
		Upper	Lower	Upper	Lower	Upper	Lower	
0.0	0.0	-0.525 92 ^c	-0.536 79 ^c	0.5	0.5	0.036 79	0.025 92	0.026 85 ^c
0.000 21	0.1	-0.525 92	-0.536 79	0.500 20	0.500 20	0.036 59	0.025 72	
0.000 5	0.235	-0.525 92	-0.536 79	0.500 49	0.500 49	0.036 30	0.025 43	0.026 35
0.001 0	0.470	-0.525 91	-0.536 79	0.500 99	0.500 99	0.035 80	0.024 92	0.025 85
0.002 13	1.0	-0.525 88	-0.536 76	0.502 11	0.502 11	0.034 65	0.023 77	
0.002 5	1.17	-0.525 87	-0.536 75	0.502 47	0.502 47	0.034 28	0.023 40	0.024 3
0.005	2.35	-0.525 72	-0.536 61	0.504 96	0.504 96	0.031 65	0.020 76	0.021 7
0.01	4.7	-0.525 10	-0.536 06	0.509 89	0.509 89	0.026 17	0.015 21	0.016 2
0.014 89	7.0	-0.524 13	-0.535 20	0.514 66	0.514 65	0.020 54	0.009 48	
0.019 14	9.0	-0.523 02	-0.534 23	0.518 77	0.518 76	0.015 46	0.004 26	
0.023 40	11.0	-0.521 67	-0.533 06	0.522 84	0.522 83	0.010 22	-0.001 16	
0.027 65	13.0	-0.520 12	-0.531 71	0.526 88	0.526 87	0.004 83	-0.006 75	

^a $\gamma = (2.127 15 \times 10^{-10} \text{ a.u./G}) B(\text{G})$.

^bR. J. W. Henry, R. F. O'Connell, Ed. R. Smith, G. Chanmugam, and A. K. Rajagopal, Ref. 18.

^cExact results for $B=0$ of C. L. Pekeris, Ref. 32, are $E(H^-) = -0.527 751$ a.u., $I(H^-) = 0.027 751$ a.u.

TABLE II. Ground-state energy of He, $E(\text{He})$, binding energy of He⁺, $I(\text{He}^+)$, and binding energy of He, $I(\text{He})$, in a uniform magnetic field.

γ^a (a.u.)	B (10 ⁸ G)	Present adiabatic Results		$E(\text{He})$ (a.u.) ^b		Coulomb Perturbation GLMO	Variational L	$I(\text{He}^+)$		$I(\text{He})^b$		Variational SHO
		Upper	Lower	Magnetic Perturbation THRSW	Hartree Fock THRSW			Upper	Lower	Upper	Lower	
0.0	0.0	-2.895 17 ^c	-2.929 67 ^c	-2.903 25	-2.861 70	-2.750 00	-2.901 45	2.0	2.0	0.929 67 ^c	0.895 17 ^c	
0.002 13	0.1	-2.895 16	-2.929 66					2.002 15	2.002 15	0.927 51	0.893 01	0.88
0.010 64	0.5	-2.895 07	-2.929 57					2.010 59	2.010 59	0.918 98	0.884 48	
0.021 27	1.0	-2.894 80	-2.929 30					2.021 14	2.021 14	0.908 16	0.873 66	0.86
0.031 91	1.5	-2.894 35	-2.928 84					2.031 63	2.031 63	0.897 21	0.862 72	
0.04	1.88	-2.893 89	-2.928 37	-2.901 95	-2.860 40			2.039 58	2.039 58	0.888 79	0.854 31	
0.05	2.35	-2.893 17	-2.927 65					2.049 34	2.049 34	0.878 31	0.843 83	0.825
0.085 09	4.0	-2.889 35	-2.923 85					2.083 26	2.083 75	0.840 59	0.806 10	
0.1	4.70	-2.887 11	-2.921 16	-2.895 25	-2.853 85	-2.743 05	-2.893 55	2.097 48	2.097 46	0.823 68	0.799 65	0.77
0.15	7.05	-2.876 89	-2.911 90					2.144 36	2.144 26	0.767 54	0.732 63	

^a $\gamma = (2.127 15 \times 10^{-10} \text{ a.u./G}) B(\text{G})$.^bLetter key to results of other authors: THRSW, Thurner, Herold, Ruder, Schlicht, and Wunner, Ref. 21; GLMO, Gadiyak, Lozovik, Mashchenko, and Obrecht, Ref. 12; L, Larsen, Ref. 11; SHO, Surnelian, Henry, and O'Connell, Refs. 19 and 20.^cExact results for $B=0$ of C. L. Pekeris, Ref. 32, are $E(\text{He}) = -2.903 72 \text{ a.u.}$, $I(\text{He}) = 0.903 72 \text{ a.u.}$

that the two electron spins are antialigned with the magnetic field, we finally obtain the following expressions for the binding energies of the *singlet* ground states with respect to the *triplet* state threshold:¹⁸⁻²⁰

$$I(\text{H}^-) = -I(\text{H}) - E(\text{H}^-), \quad (36a)$$

$$I(\text{He}) = -I(\text{He}^+) - E(\text{He}). \quad (36b)$$

In order to compute the binding energies for H⁻ and for He according to Eq. (36) we have had to compute the binding energies for the one-electron systems H and He⁺. We computed these latter binding energies according to the method of Ref. 25. We obtained rigorous upper and lower bounds on the exact binding energies.

Our upper and lower bound results for $E(\text{H}^-)$, $I(\text{H})$, and $I(\text{H}^-)$ are given in Table I. Our upper and lower bound results for $E(\text{He})$, $I(\text{He}^+)$, and $I(\text{He})$ are given in Table II. For $B=0$, our upper and lower bound results for $E(\text{H}^-)$, $I(\text{H}^-)$, $E(\text{He})$, and $I(\text{He})$ sandwich the exact results of Pekeris³² with the upper bounds on the energies and the lower bounds on the binding energies on closer agreement, as expected. For $B>0$, our upper and lower bounds on the one-electron system binding energies $I(\text{H})$ and $I(\text{He}^+)$ are essentially identical indicating that these are exactly determined. The differences between the upper and lower bounds on the two-electron system energies $E(\text{H}^-)$ and $E(\text{He})$ are thus the sole origin of the difference between the lower and upper bounds on the corresponding binding energies $I(\text{H}^-)$ and $I(\text{He})$.

The relatively few results of other authors for $I(\text{H}^-)$, $E(\text{He})$, and $I(\text{He})$ for the magnetic field strengths considered in this paper are also given in Tables I and II. In particular, Table II gives magnetic perturbation,²¹ Hartree-Fock,²¹ Coulomb perturbation,¹² and variational¹¹ results for $E(\text{He})$. Only the magnetic perturbation²¹ and variational¹¹ results lie between our lower and upper bound results. Both of these upper bound results are better than our upper bound result because of the use of more accurate wave functions to describe the correlations existing in the absence of the magnetic field. As may be verified from Table II for $\gamma=0.1$, however the *change* in $E(\text{He})$ brought about by the magnetic field is the same in all three calculations: 0.0081 a.u. (this paper), 0.0080 a.u. (Ref. 21), and 0.0079 a.u. (Ref. 11). Variational results¹⁸⁻²⁰ for $I(\text{H}^-)$ and $I(\text{He})$ compare most closely with our rigorous lower bounds for these binding energies, as shown clearly in Figs. 7 and 8. Our lower bound results for $I(\text{H}^-)$ are not quite as good as those of Ref. 18, while our lower bound results for $I(\text{He})$ are slightly better than those of Refs. 19 and 20.

V. CONCLUSIONS

Our results indicate that for magnetic field strengths $B < 10^9 \text{ G}$ such that the magnetic interactions may be treated perturbatively an adiabatic approximation in hyperspherical coordinates provides two-electron system energies and binding energies comparable to those obtained from variational calculations. Our use of oblate-

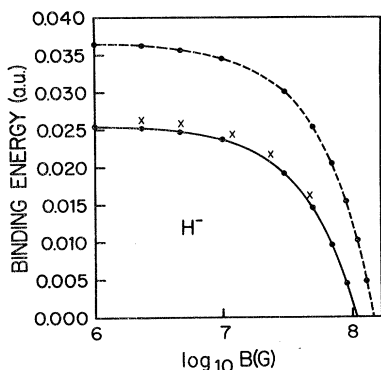


FIG. 7. Binding energy (a.u.) for the singlet ground state of H^- vs magnetic field strength. *Solid line*: present lower bound results. *Dashed line*: present upper bound results. *Crosses*: variational results of Henry *et al.* (Ref. 18).

spheroidal angle functions has permitted the representation of the hyperspherical channel function Φ_μ by only a few terms and allowed the bulk of the magnetic field induced l mixing to be represented implicitly. Worth noting is our finding that the overwhelmingly most important angular distortion of the ground-state two-electron wave function by a magnetic field is the one-electron $s \rightarrow d$ transition leading to a reduction in the ss^1S component and a corresponding increase in the sd^1D component.

APPENDIX A: MATRIX ELEMENTS APPEARING IN EQ. (26)

The matrix element of the Coulomb interaction operator C in Eq. (6) between states of the form in Eq. (24), integrated over \hat{r}_1 and \hat{r}_2 is

$$\begin{aligned}
 C_{\nu_1 \nu_2 \lambda M, \nu'_1 \nu'_2 \lambda' M} &= 2Z (\cos^{-1} \alpha + \sin^{-1} \alpha) \delta_{\nu_1 \nu'_1} \delta_{\nu_2 \nu'_2} \delta_{\lambda \lambda'} \\
 &- \frac{2}{\cos \alpha} \sum_{l=0}^{\infty} \sum_{m=-l}^{+l} \tan^l \alpha \sum_{m_1 m_2} \sum_{m'_1 m'_2} \sum'_{l_1 \geq |m_1|} \sum'_{l_2 \geq |m_2|} \sum'_{l'_1 \geq |m'_1|} \sum'_{l'_2 \geq |m'_2|} D_{l_1}^{\nu_1 m_1}(\chi) D_{l_2}^{\nu_2 m_2}(\eta) \langle \nu_1 m_1 \nu_2 m_2 | \lambda M \rangle \\
 &\quad \times D_{l'_1}^{\nu'_1 m'_1}(\chi) D_{l'_2}^{\nu'_2 m'_2}(\eta) \langle \nu'_1 m'_1 \nu'_2 m'_2 | \lambda' M \rangle \\
 &\quad \times (-1)^{m'_1 + m_2} \begin{pmatrix} l'_1 & l & l_1 \\ -m'_1 & m & m_1 \end{pmatrix} \begin{pmatrix} l_2 & l & l'_2 \\ -m_2 & m & m'_2 \end{pmatrix} \\
 &\quad \times ([l_1][l'_1][l_2][l'_2])^{1/2} \\
 &\quad \times \begin{pmatrix} l_1 & l & l'_1 \\ 0 & 0 & 0 \end{pmatrix} \begin{pmatrix} l_2 & l & l'_2 \\ 0 & 0 & 0 \end{pmatrix}, \tag{A1}
 \end{aligned}$$

where the D_l^m coefficients are defined in Eq. (21). Note that the bracket in Eq. (A1) denotes $[x] \equiv 2x + 1$.

The \underline{W} and \underline{X} matrices occur because of the α dependence [cf. Eq. (10)] of the oblate-spheroidal angle functions in Eq.

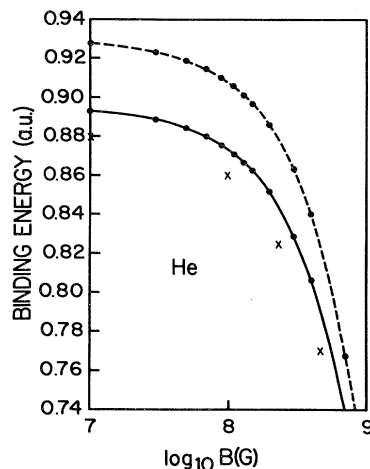


FIG. 8. Binding energy (a.u.) for the singlet ground state of He vs magnetic field strength. *Solid line*: present lower bound results. *Dashed line*: present upper bound results. *Crosses*: variational results of Surmelian *et al.* (Refs. 19 and 20).

ACKNOWLEDGMENTS

We wish to thank Professor Ronald J. W. Henry for providing us with unpublished data and Professor Robert F. O'Connell for a useful discussion. We are also grateful to Dr. Donald L. Miller for computational advice. This work was supported in part by the U.S. National Science Foundation under Grant No. PHYS-8026055.

(24). Expressions for them are

$$W_{\nu_1\nu_2\lambda,\nu'_1\nu'_2\lambda'} = 2 \sum_{m_1m_2} \langle \nu_1m_1\nu_2m_2 | \lambda M \rangle \left[\delta_{\nu_2\nu'_2} \left[g_{\nu_1m_1}, \frac{\partial g_{\nu'_1m_1}}{\partial \alpha} \right] + \delta_{\nu_1\nu'_1} \left[g_{\nu_2m_2}, \frac{\partial g_{\nu'_2m_2}}{\partial \alpha} \right] \right] \langle \nu'_1m_1\nu'_2m_2 | \lambda' M \rangle, \quad (\text{A2})$$

$$X_{\nu_1\nu_2\lambda,\nu'_1\nu'_2\lambda'} = \sum_{m_1m_2} \langle \nu_1m_1\nu_2m_2 | \lambda M \rangle \left[\delta_{\nu_2\nu'_2} \left[g_{\nu_1m_1}, \frac{\partial^2 g_{\nu'_1m_1}}{\partial \alpha^2} \right] + \delta_{\nu_1\nu'_1} \left[g_{\nu_2m_2}, \frac{\partial^2 g_{\nu'_2m_2}}{\partial \alpha^2} \right] \right. \\ \left. + 2 \left[g_{\nu_1m_1}, \frac{\partial g_{\nu'_1m_1}}{\partial \alpha} \right] \left[g_{\nu_2m_2}, \frac{\partial g_{\nu'_2m_2}}{\partial \alpha} \right] \right] \langle \nu'_1m_1\nu'_2m_2 | \lambda' M \rangle. \quad (\text{A3})$$

APPENDIX B: FIRST-ORDER APPROXIMATIONS

The matrices in Appendix A simplify significantly in the approximation that $\lambda = \lambda' = M = 0$ and that only terms that are first order in the Δ_l^m [cf. Eq. (27)] are kept. The results are

$$C_{\nu_1\nu_20,\nu'_1\nu'_20} = 2Z(\cos^{-1}\alpha + \sin^{-1}\alpha) \delta_{\nu_1\nu'_1} \delta_{\nu_1\nu_2} \delta_{\nu'_1\nu'_2} - \frac{2\delta_{\nu_1\nu_2} \delta_{\nu'_1\nu'_2}}{\cos\alpha} (2\nu_1+1)^{1/2} (2\nu'_1+1)^{1/2} \\ \times \sum_{l=0}^{\infty} (-1)^l \tan^l \alpha \begin{pmatrix} \nu_1 & l & \nu'_1 \\ 0 & 0 & 0 \end{pmatrix}^2 [1 + \bar{\Delta}_{\nu_1}^{\nu_1}(\chi) + \bar{\Delta}_{\nu_1}^{\nu_1}(\eta) + \bar{\Delta}_{\nu'_1}^{\nu'_1}(\chi) + \bar{\Delta}_{\nu'_1}^{\nu'_1}(\eta)], \quad (\text{B1})$$

$$W_{\nu_1\nu_20,\nu'_1\nu'_20} = 0, \quad (\text{B2})$$

$$X_{\nu_1\nu_20,\nu'_1\nu'_20} = \delta_{\nu_1\nu_2} \delta_{\nu'_1\nu'_2} \delta_{\nu_1\nu'_1} 4\chi\eta \left[\frac{\partial^2 \bar{\Delta}_{\nu_1}^{\nu_1}(\chi)}{\partial \chi^2} + \frac{\partial^2 \bar{\Delta}_{\nu_1}^{\nu_1}(\eta)}{\partial \eta^2} \right]. \quad (\text{B3})$$

In the above equations we have introduced the following notation:

$$\bar{\Delta}_\nu^{\nu} \equiv \frac{1}{2\nu+1} \sum_{m=-\nu}^{+\nu} \Delta_\nu^{m\nu}. \quad (\text{B4})$$

¹R. H. Garstang, Rep. Prog. Phys. **40**, 105 (1977).

²C. W. Clark, K. T. Lu, and A. F. Starace, in *Progress in Atomic Spectroscopy, Part C*, edited by H. J. Beyer and H. Kleinpoppen (Plenum, New York, 1984), pp. 247–320.

³R. H. Garstang, J. Phys. (Paris), Colloq. **43**, C2-19 (1982).

⁴H. Hasegawa, in *Physics of Solids in Intense Magnetic Fields*, edited by E. D. Haidemenakis (Plenum, New York, 1969), Chap. 10.

⁵R. F. O'Connell, J. Phys. (Paris), Colloq. **43**, C2-81 (1982).

⁶R. Cohen, J. Lodenquai, and M. Ruderman, Phys. Rev. Lett. **25**, 467 (1970).

⁷M. Ruderman, in *Physics of Dense Matter*, edited by C. J. Hansen (Reidel, Boston, 1972), pp. 117–131.

⁸A. R. P. Rau, R. O. Mueller, and L. Spruch, Phys. Rev. A **11**, 1865 (1975).

⁹R. O. Mueller, A. R. P. Rau, and L. Spruch, Phys. Rev. A **11**, 789 (1975).

¹⁰J. Virtamo, J. Phys. B **9**, 751 (1976).

¹¹D. M. Larsen, Phys. Rev. B **20**, 5217 (1979).

¹²G. V. Gadiyak, Yu. E. Lozovik, A. I. Mashchenko, and M. S. Obrecht, Phys. Lett. **87A**, 18 (1981).

¹³P. Pröschel, W. Rösner, G. Wunner, H. Ruder, and H. Herold, J. Phys. B **15**, 1959 (1982).

¹⁴R. H. Garstang and S. B. Kemic, in *The Structure of Matter*,

edited by B. G. Wybourne (U. Canterbury, New Zealand, 1972), pp. 396–404.

¹⁵R. H. Garstang and S. B. Kemic, Astrophys. Space Sci. **31**, 103 (1974).

¹⁶S. B. Kemic, Astrophys. J. **193**, 213 (1974).

¹⁷S. B. Kemic, "Wavelengths and Strengths of H and He Transitions in Large Magnetic Fields," JILA Report No. 113, April 15, 1974 (University of Colorado, Boulder) (unpublished).

¹⁸R. J. W. Henry, R. F. O'Connell, Ed. R. Smith, G. Chanmugam, and A. K. Rajagopal, Phys. Rev. D **9**, 329 (1974); numerical values for $I(\text{H}^-)$ provided by R. J. W. Henry (private communication).

¹⁹Garabed Leon Surmelian, Ph.D. thesis, Louisiana State University, 1974 (available through University Microfilms International, Ann Arbor, Michigan, Order No. 75-1954).

²⁰G. L. Surmelian, R. J. W. Henry, and R. F. O'Connell, Phys. Lett. **49A**, 431 (1974).

²¹G. Thurner, H. Herold, H. Ruder, G. Schlicht, and G. Wunner, Phys. Lett. **89A**, 133 (1982).

²²J. Macek, J. Phys. B **1**, 831 (1968).

²³A. F. Starace, in *Physics of Electronic and Atomic Collisions*, edited by S. Datz (North-Holland, Amsterdam, 1982), pp. 431–446.

- ²⁴U. Fano, Rep. Prog. Phys. 46, 97 (1983).
- ²⁵A. F. Starace and G. L. Webster, Phys. Rev. A 19, 1629 (1979).
- ²⁶C. Flammer, *Spheroidal Wave Functions* (Stanford University, Stanford, Calif. 1957).
- ²⁷M. Abramowitz and I. A. Stegun, *Handbook of Mathematical Functions* (Dover, New York, 1965).
- ²⁸H. A. Bethe and E. E. Salpeter, *Quantum Mechanics of One- and Two-Electron Atoms* (Springer, Berlin, 1957), Secs. 45–50.
- ²⁹In this paper we assume the nucleus to be infinitely massive. J. E. Avron, I. W. Herbst, and B. Simon, Ann. Phys. 114, 431 (1978), have examined the separability of center-of-mass motion for N charged particles in a uniform magnetic field.
- ³⁰P. M. Morse and H. Feshbach, *Methods of Theoretical Physics* (McGraw-Hill, New York, 1953), Vol. II, pp. 1730–1.
- ³¹L. D. Landau and E. M. Lifshitz, *Quantum Mechanics*, 2nd ed. (Addison-Wesley, Reading, Mass., 1965), Chap. XV.
- ³²C. L. Pekeris, Phys. Rev. 126, 1470 (1962).